

Chapter 19

Second Harmonic Imaging of Membrane Potential

Leslie M. Loew and Aaron Lewis

Abstract The non-linear optical effect known as second harmonic generation (SHG) has been recognized since the earliest days of the laser. But it has only been in the last 20 years that it has begun to emerge as a viable microscope imaging contrast mechanism for visualization of cell and tissue structure and function. This is because only small modifications are required to equip a standard laser scanning 2-photon microscope for second harmonic imaging microscopy (SHIM). SHG signals from certain membrane-bound dyes are highly sensitive to membrane potential, indicating that SHIM may become a valuable probe of cell physiology. However, for the current generation of dyes and microscopes, the small signal size limits the number of photons that can be collected during the course of a fast action potential. Better dyes and optimized microscope optics could ultimately lead to the ability to image neuronal electrical activity with SHIM.

Keywords Fluorescence • Non-linear optics • Membrane potential • Voltage sensor • Electrochromism • Chemistry • Optics • 2-Photon • Microscopy • Imaging • SHG

1 Introduction and Overview

SHG, also called “frequency doubling”, is a non-linear optical process that has been known since the earliest days of laser physics. This phenomenon requires intense laser light passing through a highly polarizable material with a non-centrosymmetric molecular organization. The emerging light is at precisely half the wavelength (or twice the frequency) of the light that entered the material. The most common application of SHG in laser optics is to produce visible laser light from an infrared

L.M. Loew (✉)

Department of Cell Biology, R. D. Berlin Center for Cell Analysis and Modeling,
University of Connecticut Health Center, Farmington, CT 06030-1507, USA
e-mail: les@volt.uchc.edu

A. Lewis

Department of Applied Physics, Hebrew University, Jerusalem, Israel
e-mail: LEWISU@vms.huji.ac.il

© Springer International Publishing Switzerland 2015

M. Canepari et al. (eds.), *Membrane Potential Imaging in the Nervous System and Heart*, Advances in Experimental Medicine and Biology 859,
DOI 10.1007/978-3-319-17641-3_19

473

laser; the SHG material for such an application is an inorganic crystal placed in the light path immediately following the primary laser. As in the case of two-photon excitation, the probability of producing SHG is proportional to the square of the incident light intensity. Therefore, when incorporated into a microscope, it has the same intrinsic optical sectioning attributes as two-photon excited fluorescence (2PF) microscopy.

The idea that 2PF and SHG might each be used for microscopy was first proposed by Sheppard (Sheppard et al. 1977). The first biological SHG microscopy experiments were by Freund et al. in 1986 (Freund et al. 1986). They utilized SHG to study the orientation of collagen fibers in rat tail tendon at approximately 50 μm resolution and showed the collagen fibers formed highly dipolar structures on this size scale. Our work focused from the start on the possibility that electrochromic membrane dyes could produce SHG. We first showed that the styryl dyes such as di-4-ANEPPS, which had been developed for voltage sensing via fluorescence, could produce strong SHG when arrayed in a monolayer (Huang et al. 1988). We then measured the second harmonic response of styryl dyes to membrane potential on a model membrane system (Bouevitch et al. 1993) and demonstrated the possibility of imaging live cells by SHG (Ben-Oren et al. 1996). In all this earlier work, stage scanning with a picosecond laser source focused through the microscope was used and frame rates of minutes to hours were required. The application of mode-locked lasers to 2PF microscopy was demonstrated in 1990 by Denk, Strickler and Webb (Denk et al. 1990), making non-linear optical microscopy a practical tool for cell biology and physiology. We were able to apply scanning of mode-locked lasers to produce the first high resolution SHG microscopy images of cells acquired with frame rates of seconds (Campagnola et al. 1999). The use of SHIM to investigate membrane potential is the primary focus of this chapter, but it should also be noted that the use of SHIM to investigate collagen and other endogenous biological assemblies has mushroomed in the last 10 years and is widely being investigated for clinical diagnostic applications (Bianchini and Diaspro 2008; Campagnola and Loew 2003; Mohler et al. 2003).

Since SHG is a non-linear optical phenomenon, it shares many of the features of 2PF microscopy. But it is critical to appreciate the differences. While 2PF involves the absorption of two photons to excite a fluorophore, followed by relaxation and fluorescence emission, SHG is a process in which two photons are directly converted into a single photon of twice the energy. SHG light retains the coherence of the fundamental laser beam, while the fluorescence from 2PF is no longer coherent. Furthermore, SHG should be considered a material property rather than a molecular property. It requires a distribution of "harmonophores" that lacks a center of symmetry; this constraint is readily satisfied at cellular membranes in which SHG-active constituents are unevenly distributed between the two leaflets of the lipid bilayer. However, dyes bound to highly convoluted membranous structures such as the endoplasmic reticulum do not produce SHG; this is because the orientations of the dye molecules are random on the spatial scale of the wavelength of light, thus violating the requirement for a noncentrosymmetric distribution of harmonophores. Finally, a key difference is that fluorescence intensity is linearly

related to the concentration of fluorophores, while SHG is quadratically dependent on the density of harmonophores.

SHG does not involve excitation of molecules into an excited state. Thus, it might be expected that photobleaching and phototoxicity of live specimens should be eliminated. However, there can be collateral damage if the incident laser light also produces 2-photon excitation of chromophores in the specimen. Electrochromic membrane dyes can be used to produce SHG that is sensitive to membrane potential. This promises to enable new optical approaches to mapping electrical activity in complex neuronal systems. Excitation uses near infrared wavelengths, allowing excellent depth penetration, and hence this method is well-suited for studying thick tissue samples such as brain slices or in vivo brain imaging. Additionally, 2PF images can be collected in a separate data channel simultaneously with SHG, permitting the simultaneous imaging of membrane potential and the distribution of fluorescent labels. Ratiometric SHG:2PF techniques allow for the quantitation of chiral-enhancement and voltage-sensitivity, while normalising out irrelevant parameters arising from laser fluctuations, sample movement and non-uniform staining (Campagnola et al. 1999). However, a major challenge that will be discussed is the small flux of SHG photons from the current generation of membrane staining voltage-sensitive dyes.

The rest of this chapter will be devoted to more detailed discussions of many of these points. We will also provide guidance on how to set up an SHIM experiment and review some of the attempts to use SHIM for voltage imaging.

2 The Photophysics of SHG

An energy diagram (also known as a Jablonski diagram) will help us to understand what happens to the incident light during the process of fluorescence and SHG. Figure 19.1 contrasts the energetics of 1 and 2 photon fluorescence and SHG. For one photon fluorescence, the energy of the photon (blue arrow) matches the gap between the ground state (GS) and a sublevel within the excited state (ES), which is composed of a manifold of electronic and vibrational states. This initial excited state rapidly relaxes to the lowest energy state of the ES manifold, losing some energy to heat in the process. The ES has an average lifetime of Δt (on the order of ns) before relaxing back to the GS by emitting a fluorescent photon. Because there is always time for relaxation of the excited state, usually involving vibrational relaxation and solvent reorganization, the wavelength of the emitted fluorescence is always longer (i.e. lower energy) than the absorbed photon. For 2PF (center of Fig. 19.1), the wavelength of the exciting light is approximately twice that of the corresponding 1 photon absorption process; under these circumstances 2 photons (represented by two red arrows in the figure) are required to deliver sufficient energy for excitation to the ES manifold; this has a much lower probability and therefore requires light of much higher intensity (i.e. photon flux) than 1 photon absorption. Because 2 photons are involved, the probability of absorption is

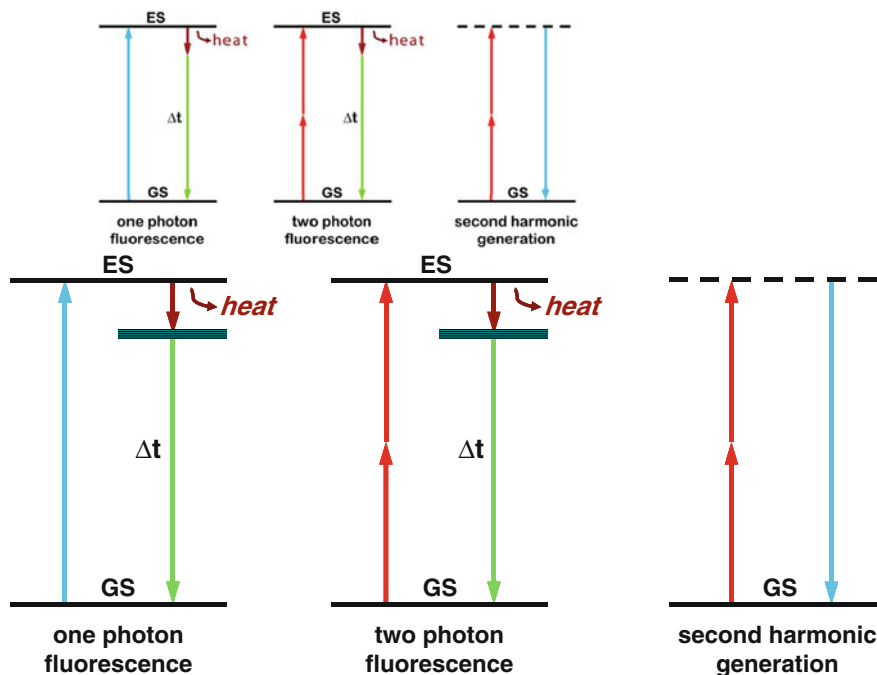


Fig. 19.1 Jablonski diagrams for 1 photon fluorescence, 2PF and SHG. GS = ground state; ES = excited state; Δt = excited state lifetime

proportional to the square of the incident light intensity. But once the molecule reaches the ES, it does not retain a memory of where it came from and it behaves exactly as described for 1 photon excitation. SHG, shown on the right of Fig. 19.1, does not involve an excited state and is an instantaneous transformation of 2 photons (the red arrows) into a single photon with precisely twice the energy (or half the wavelength), represented by the blue arrow pointing downwards. Importantly, there is no excited state involved in SHG and the light that is produced retains the coherence of the incident fundamental laser light.

To explore the origin of SHG requires consideration of how the light interacts with the non-linear optical material. A qualitative approach will provide a physical understanding of the process and why it is fundamentally so different from fluorescence. Much as when a guitar string is plucked too hard, if an intense pulse of light interacts with a material, it can interact with the electrons in that material and emerge with additional harmonics. The ability of the oscillating electric field in the light wave to interact with the material depends on its polarisability. We can understand how this might produce harmonics of the original fundamental frequency by referring to Fig. 19.2. A high amplitude electromagnetic wave impinges on an array of molecules that are oriented with their electron clouds aligned so as to reinforce the light wave for the positive component of the oscillating electric field and oppose the negative electric field component. The emerging electromagnetic

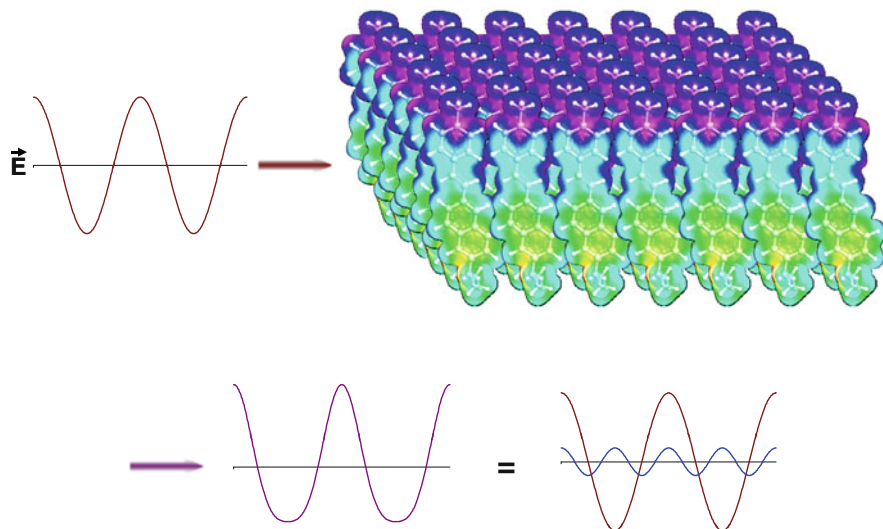


Fig. 19.2 Qualitative picture of the optical physics underlying SHG. The oscillating electric field of the intense fundamental light beam (*red sine wave on the top left*) impinges on an ordered array of polarizable molecules. The interaction of the oscillating wave with the material induces a distortion of the emergent light wave (*violet, bottom left*), that is equivalent to the mixing of the original fundamental frequency with a small contribution from twice the frequency, i.e. the second harmonic (shown in *blue on the bottom right*). The molecular array shown in the *upper right* was created by 2D translations of an electron density map of the aminonaphthylethenylpyridinium (ANEP) chromophore. The electron density map was rendered in *colors* from the output of molecular orbital calculations

wave is correspondingly distorted and can be decomposed into components that correspond to the fundamental frequency plus a component at double that frequency. It is apparent from this simple picture that SHG depends on the collective properties of the array; this distinguishes it from absorbance and fluorescence, which depend on the interaction of photons with individual molecules. Reference to Fig. 19.2 makes it easy to understand why a fully centrosymmetric array of molecules or randomly oriented molecules in a homogeneous solution cannot produce SHG: it is because the electric field vector of the fundamental light wave would not be differentially distorted, as it is in Fig. 19.2 for an ordered array. One can also appreciate from this picture that the SHG will depend strongly on the polarization of the incoming light and its angle of incidence with respect to the array of harmonophores in the non-linear optical material—i.e. tensor relationships. Thus while this simple picture cannot fully describe the details of SHG, it nicely explains many qualitative features of the phenomenon.

With this qualitative picture in hand, it is worthwhile to consider the photophysics at a more rigorous level in order to appreciate some of the more subtle features of SHG and how it differs from 2PF. Such a treatment necessarily begins with the general expression for polarisability, which can be expressed as a

Taylor series in the electric field: $\mathbf{P} = \chi^{(1)} \otimes \mathbf{E} + \chi^{(2)} \otimes \mathbf{E} \otimes \mathbf{E} + \chi^{(3)} \otimes \mathbf{E} \otimes \mathbf{E} \otimes \mathbf{E} + \dots$

\mathbf{P} is the induced polarisation vector, \mathbf{E} represents the vector electric field, $\chi^{(i)}$ is the i th-order non-linear susceptibility tensor and \otimes represents a combined tensor product and integral over frequencies. It is again important to emphasize that the $\chi^{(i)}$ are bulk properties of the material. However, they parallel the interaction of an electric field with molecules based on the molecular properties, respectively, of dipole moment, and polarizability and hyperpolarisabilities (Cole and Kreiling 2002; Moreaux et al. 2000a; Williams 1984). The first term in the series describes normal absorption and reflection of light. The second- and third-order terms correspond to the phenomena of SHG and 2PF and their sensitivity to electric field. To begin to appreciate how SHG might directly depend on the electric field associated with the membrane potential in addition to the oscillating electric field of the light, one can decompose the above equation into a combination of a true second-order process and a third-order process dependent on a constant electric field:

$$\mathbf{P} = \chi^{(2)} \otimes \mathbf{E}(\omega) \otimes \mathbf{E}(\omega) + \chi^{(3)} \otimes \mathbf{E} \otimes \mathbf{E}(\omega) \otimes \mathbf{E}(\omega) \quad (19.1)$$

$$\mathbf{P} = \chi^{(2)}_{\text{eff}}(\mathbf{E}) \otimes \mathbf{E}(\omega) \otimes \mathbf{E}(\omega) \quad (19.2)$$

Here, $\chi^{(2)}_{\text{eff}}(\mathbf{E})$ is an effective second-order non-linear susceptibility (Conboy and Richmond 1997; Yan et al. 1998) that depends on a static electric field vector, \mathbf{E} . This term could impart a membrane potential sensitivity for harmonophores embedded on one side of a cell membrane.

The SHG intensity, $I(2\nu)$, is related to the square of the second order non-linear susceptibility, $\chi^{(2)}$ (or $\chi^{(2)}_{\text{eff}}(\mathbf{E})$):

$$I(2\nu) \propto \frac{[\chi^{(2)} I(\nu)]^2}{\tau} \quad (19.3)$$

where $I(\nu)$ is the laser pulse energy, ν is the fundamental frequency and 2ν is the second harmonic frequency. As in 2PF, the signal has a quadratic dependence on laser intensity and an inverse dependence on pulsewidth, τ , but since SHG is an instantaneous process, signal will only be generated during the duration of the laser pulse.

We now turn to a consideration of the molecular origin of SHG. $\chi^{(2)}$ is related to the molecular property β , the first hyperpolarizability according to:

$$\chi^{(2)} = N_s \langle \beta \rangle \quad (19.4)$$

where N_s is the density of molecules and the brackets denotes an orientational average. This further underscores the need for a non-centrosymmetric region, since $\langle \beta \rangle$ would vanish for an isotropic distribution. Examination of Eqs. (19.3) and

(19.4) also reveals a major difference in the expected contrast for the 2PF and SHG signal levels: SHG depends on the square of the surface density whereas fluorescence intensity is linear with the density of fluorophores. This can lead to significant differences in these two mechanisms even when signal arises from the same dye in the membrane. For example, at high dye concentrations the fluorescence signal will become quenched due to dye aggregation and subsequent non-radiative decay, while the SHG would actually be larger due to the square dependency on the surface density. SHG can be resonance-enhanced when the second harmonic transition overlaps with an electronic absorption band. The resonance-enhanced molecular hyperpolarizability (Dirk et al. 1986; Morley 1988; Nicoud and Twieg 1987), which determines the resonance contribution, is given by:

$$\beta = \frac{4\mu_{eg}^2(\mu_e - \mu_g)}{3h^2(\nu_{eg}^2 - \nu^2)(\nu_{eg}^2 - 4\nu^2)} \quad (19.5)$$

Where h is Planck's constant, μ_g and μ_e are the dipole moments of the ground and excited states, respectively, μ_{eg} is the transition moment, ν is the frequency of the incident light, and $h\nu_{eg}$ is the energy for the electronic transition from the ground to the excited state. For the very broad absorption bands of organic dyes in solution, the resonance condition where 2ν overlaps ν_{eg} will pertain over a large range of wavelengths. Other consequences of this simple expression are that β is enhanced when there is a large difference in the ground and excited state electron distribution, i.e. a large $\mu_e - \mu_g$, and when the dye has a large extinction coefficient (which is proportional to μ_{eg} , the transition dipole). These are precisely the features that have been behind the design of our electrochromic styryl dyes and this is what led us to initially explore the possibility that they may produce large SHG signals. This relationship between SHG and electrochromism manifest in Eqs. (19.2) and (19.5) was also the original motivation for us to explore whether SHG from membranes stained with our dyes could be sensitive to membrane potential.

3 SHG Response to Membrane Potential

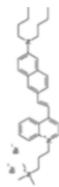
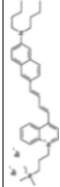
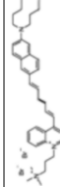
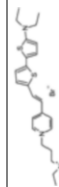
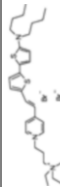
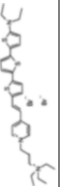
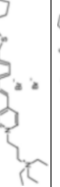
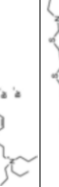
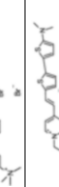
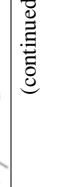
Our first foray into the non-linear optical properties of our dyes, involved creating a monolayer of di-4-ANEPPS in a Langmuir-Blodgett trough (Huang et al. 1988). In a series of papers that culminated in the first high resolution SHG images (Ben-Oren et al. 1996; Bouevitch et al. 1993; Campagnola et al. 1999), we were able to show that the SHG signal from ANEP dye stained membranes is sensitive to membrane potential. These experiments were continued (Campagnola et al. 2001; Clark et al. 2000; Millard et al. 2003a, b, 2004, 2005a, b; Teisseyre et al. 2007; Yan et al. 2006) and were validated and extended by the laboratories of Jerome Mertz, Rafael Yuste, Kenneth Eisenthal and Watt Webb (Araya et al. 2006, 2007;

Dombeck et al. 2004, 2005; Jiang et al. 2007; Moreaux et al. 2000a, b, 2003; Nuriya et al. 2006; Pons et al. 2003).

Table 19.1, taken from a published paper (Teisseyre et al. 2007), summarizes results from a series of very promising new probes for both fluorescence and SHG. The absorbance and emission maxima in this Table are for dyes bound to lipid vesicles. The first three dyes in the Table are noteworthy because of the huge fluorescence sensitivities observed for them on the voltage clamped hemispherical bilayer (column 4; see Chap. 2 in this volume). Versions of these chromophores have been extraordinarily successful in fluorescence optical recording from brain slice and heart studies. A completely new class of hemicyanines employing an amino-thiophene donor moiety are the “PY” probes (for their inventor, Ping Yan) in the Table. We had employed thiophenes as linker moieties for many years, but this is the first set of hemicyanine chromophores that we are aware of where amino-thiophenes serve as the electron donor. The rationale for this donor moiety is that the thiophene behaves more like a rigidified diene than an aromatic heterocycle; thus through conjugation of the unshared electrons on the amino nitrogen is more effective than for the aniline and amino-naphthalene donor moieties in the earlier generation of dyes. Indeed, the spectra of these dyes are much further red shifted than comparable dyes employing aniline or amino-naphthalene donors. We also felt that these dyes should be particularly suitable for SHG imaging because the thiophenes are highly polarizable; additionally there should be a large change in dipole moment in going from ground to excited state for resonance enhanced SHG (Eq. 19.5). All of the dyes have absorbance maxima in the range of 530–560 nm in lipid membranes. This makes them ideal for SHG with our 1,064 nm femtosecond fiber laser and these dyes do indeed show strong SHG and the best SHG sensitivity to potential that we know of (PY-1278 is twice as good as FM-4-64). Also very striking is the 2-photon result shown for PY-1268 of 16.6 %/50 mV. It should be noted that all the results reported in columns 6 and 7 were for excitation with the 1,064 nm laser and emission at the 2 wavelength ranges indicated; no attempt was made to find optimal wavelengths for the 2PF sensitivity to potential, so most of these numbers are likely to be improvable. Indeed the 1-photon wavelength optima are generally quite different. A full account of the synthesis of this novel class of dyes has been published (Yan et al. 2008). A major problem that will need to be addressed for these dyes before they can be truly useful VSDs is their poor photostability (Zhou et al. 2007).

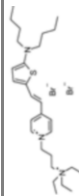
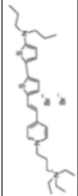
The labs of Rafael Yuste and Ken Eisenthal at Columbia U. have collaborated to perform SHG measurements of FM-4-64 applied to single neocortical pyramidal neurons through a patch pipette. FM-4-64 is a hemicyanine dye similar to our first generation styryl dyes in that it contains an aniline donor moiety (rather than an aminonaphthalene) conjugated via a trienyl linkage to a pyridinium acceptor. It has found extensive utility as a probe for synaptic vesicle cycling because it can be applied to preparations from the outside and readily becomes internalized in the vesicles. When applied from the inside, as in the Columbia experiments, the dye remains in the neuron because of its doubly positive charge; i.e. the negative resting potential of the cell will hold this relatively water soluble dye in the interior of the

Table 19.1 Linear and non-linear responses of Gen3 dyes

Dye	IPF Abs. Max (nm)	IPF Em. Max (nm)	IPF Change ($\Delta F/F$ - 100 mv); Ex/Em (nm)	SHG Change (%/50 mV)	2PF Change (%; 615 - 665 nm/50 mV)	2PF Change (%; 750 - 850 nm/50 mV)	SHG Kinetics (ms)	Structure
JPW-6008 di-4-ANEQPO	528	670	1.2E-001; 610/>665	3.84 \pm 0.38	0.79 \pm 0.37	5.03 \pm 0.26	76 \pm 13	
JPW-6003 di-4-ANBDQPO	539	708	2.0E-001; 618/>715	3.55 \pm 0.55	-6.61 \pm 0.88	4.32 \pm 0.57	<5	
JPW-6027 di-4-ANHTQPO	504	655	5.4E-002; 630/>715	4.15 \pm 0.28	-7.51 \pm 0.73	2.83 \pm 0.45	34 \pm 3	
PY-1261	547	686	5.0E-002; 625/>715	9.56 \pm 0.42	-2.57 \pm -0.24	5.22 \pm 0.28	<5	
PY-1266	552	694	1.0E-001; 635/>715	3.75 \pm 0.33	-4.80 \pm 0.53	2.25 \pm 0.47	23 \pm 2	
PY-1268	535	714	4.2E-002; 640/>715	1.82 \pm 0.18	-16.64 \pm 0.85	-4.28 \pm 0.54	<5	
PY-1274	551	691	5.0E-002; 620/>715	5.65 \pm 0.45	-4.20 \pm 0.13	3.12 \pm 0.18	-	
PY-1278	555	688	7.9E-002; 640/>715	10.70 \pm 0.59	-3.86 \pm 0.53	6.52 \pm 0.76	<5	
PY-1280	547	690	1.1E-001; 640/>715	10.13 \pm 0.88	-6.12 \pm 0.87	5.77 \pm 1.22	109 \pm 30	
PY-1282	530	676	8.0E-002; 640/>715	11.64 \pm 0.60	0.29 \pm 0.39	8.78 \pm 1.08	16 \pm 1	

(continued)

Table 19.1 (continued)

Dye	IPF Abs. Max (nm)	IPF Em. Max (nm)	IPF Change (ΔF /F - 100 mv); Ex/Em (nm)	SHG Change (%/50 mV)	2PF Change (%/615 - 665 nm/50 mV)	2PF Change (%/750 - 850 nm/50 mV)	SHG Kinetics (ms)	Structure
PY-1284	536	588	1.5E-002; 555/>610	6.18 \pm 0.68	6.72 \pm 0.58	-	-	
PY-1286	547	692	1.8E-001; 640/>715	8.09 \pm 0.42	-5.65 \pm 0.50	3.51 \pm 0.66	27 \pm 1	

dendrite, where vesicle cycling is presumably non-existent. The Columbia group has published two papers in which they used SHG to measure electrical activity in individual spines (Araya et al. 2006; Nuriya et al. 2006) and they have used this and less direct experiments (Araya et al. 2007) to argue that the spine is indeed an electrical compartment.

Gaining an understanding of the mechanism(s) by which the SHG intensity responds to membrane potential changes will, of course, allow us to design better SHG-based voltage sensors to fully exploit this new modality for optical electrophysiology. The theory of SHG, which was outlined in the previous section, provides a basis for a purely electronic mechanism by which SHG could respond to electric field. Specifically, Eqs. (19.1) and (19.2) show how a DC electric field can cause mixing of a $\chi^{(3)}$ contribution into the second order susceptibility that is responsible for SHG; Eq. (19.5) suggests that resonance enhancement of SHG depends on a large charge redistribution between the ground and excited states; an electric field should produce a second order effect on this charge redistribution. Such a purely electronic mechanism would necessarily be instantaneous on the timescale of an action potential. Although there has been some investigation of the mechanism by which SHG from the styryl dyes is sensitive to membrane potential that suggests a purely electronic mechanism (Campagnola and Loew 2003; Jiang et al. 2007; Pons et al. 2003), kinetic data, showing non-instantaneous responses, are inconsistent with this explanation (Millard et al. 2005a; Teisseyre et al. 2007).

We have shown that several of our dyes show large potential dependent changes in SHG (as high as 38 %/100 mV for di-4-ANEPPS), with some instantaneous responders, within the limits of our 5 ms time resolution, but others with response times in the tens of milliseconds (Millard et al. 2005a; Teisseyre et al. 2007). A non-instantaneous response precludes a purely electronic mechanism and suggests some form of conformational change or reorientation is involved in the mechanism of the SHG response. What is particularly curious is that in 2PF mode, which we also measured, all of the dyes showed rapid responses (consistent with the putative electrochromic mechanism for the 1PF voltage sensitivity). However in some of the kinetic traces there is a small slow component to the 2PF response that may have the same time course as the slow SHG response; Fig. 19.3, taken from Millard et al. (2005), shows a pair of kinetic traces for di-4-ANEPPS that is the best example of this behavior. Thus, it would appear that whatever molecular motion underlies the slow SHG response does not strongly affect the 2PF. We also showed that the dye responses to potential are linear and have a shallow wavelength dependence that peaks around the optimal second harmonic resonance with the 1 photon absorbance spectrum (Millard et al. 2003b, 2004, 2005a). The Mertz lab showed that a styryl quinolinium dye, di-6-APEQBS (our lab calls the same dye di-6-ASQBS (Fluhler et al. 1985)), displays a mixture of a relatively weak (3 %/100 mV) electronic response and a stronger (−12 %/100 mV) reorientation response (Pons et al. 2003). They dissected these mechanisms by analyzing the polarization dependence of the voltage response. Interestingly, both of these responses were linear and fast, but in opposite directions. The Eiesenthal-Yuste collaboration at Columbia U. recently looked at the kinetics and polarization

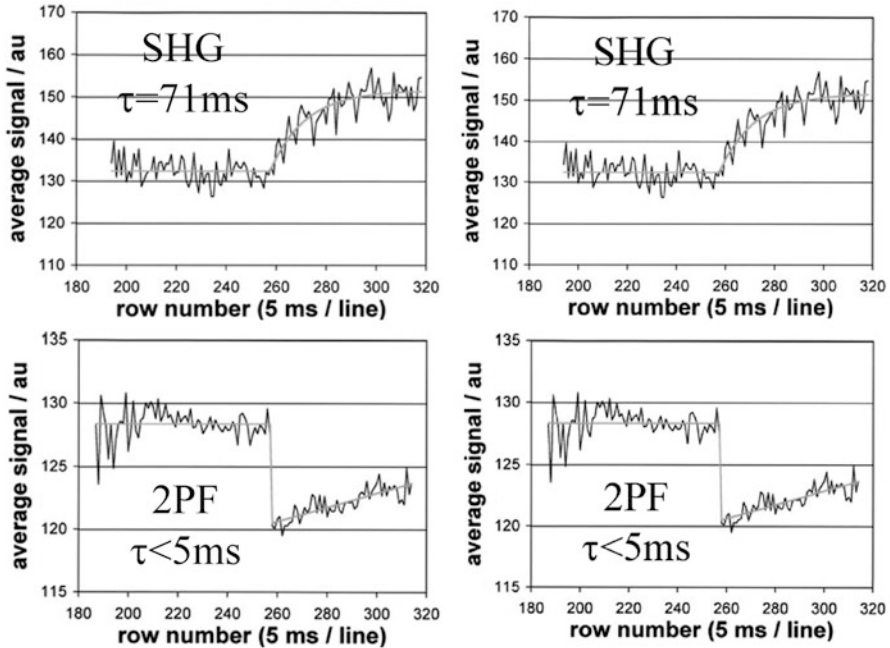


Fig. 19.3 Kinetic response to a 50 mV step of non-linear optical signals on patch clamped di-4-ANEPPS stained neuroblastoma cells. The voltage is changed at the midpoint of the trace. The 2PF signal shows an immediate decrease in fluorescence followed by a slow increase. See Millard et al. (2005), for details. Reprinted with Permission of the Journal of Membrane Biology

dependence of the 14 %/100 mV FM-4-64 SHG response (Jiang et al. 2007). They reported fast kinetics, linear voltage dependence and no change in polarization following a voltage step. By process of elimination, they concluded that the mechanism was purely electronic. However, a recent study of FM-4-64 in HEK cells (Theer et al. 2011) showed similar voltage sensitivity but a slow voltage response kinetics. The discrepancy in the kinetics between these results may be because different cell types were used, but it is clear that the voltage response mechanism of FM-4-64 can, at least in part, involve a change in its association with the plasma membrane.

It is important to emphasize that a mechanism that involves a rapid redistribution of harmonophores from a random and therefore SHG-silent population, to a well ordered non-centrosymmetric array within the membrane could produce an increase in SHG intensity without any change in its polarization. This will be the result if both states are populated both before and after the voltage change, with the voltage change effecting a change in the equilibrium between them. Based on the experiments carried out by us and by the other labs, this mechanism would be indistinguishable from what has been termed “electronic” or “electrooptic”. Our hypothesis is that the mechanism that leads to the slow voltage sensitive responses could also pertain to the SHG probes that have faster kinetics. All that is required to

produce the faster kinetics is that the rearrangement rate be increased by about a factor of 100 from the dye with the slowest response (PY1280, Table 19.1). In terms of the free energy barrier, this corresponds to a rather small difference of 2.8Kcal/mol. In fact, comparing PY-1280, with a SHG time constant of 110 ms, to PY-1261, which has a time constant of <5 ms, the only difference in the structure is a trimethylammonium vs. a triethylammonium headgroup. *Despite the difference in kinetics, these 2 dyes have virtually identical SHG sensitivities to potential (20 %/100 mV)!* Clearly the dye with the slow kinetics cannot be using an “electrooptic” mechanism and it would be surprising if the change from methyl to ethyl substituents could switch the mechanism. Our ability to synthesize many of these dyes and then compare their voltage-dependent non-linear optical properties (e.g. Fig. 19.4 and other similar comparisons in Teisseyre et al. (2007)), will be our most important tool in uncovering the mechanism(s) of the voltage sensitivity.

Happily, as can be seen from Table 19.1, we discovered that some of the more sensitive SHG dyes also displayed fast kinetics. These fast SHG dyes are also more sensitive to potential than FM-4-64. Not included in Table 19.1 is the kinetic response of the dyes in 2PF mode; interestingly, all the dyes responded with fast kinetics (i.e. faster than the 5 ms resolution of our measurement) and some of the 2PF responses are truly huge. Considering that we have not attempted to find optimal wavelengths for these dyes, using 1,064 nm excitation and just two fixed choices of emission filters, it is likely that these dyes will produce even better sensitivities than those listed in Table 19.1. But there are some new problems as already discussed regarding the poor photostability of some of the PY dyes (Zhou et al. 2007). Efforts to synthesize and characterize new SHG dyes will ultimately lead to an understanding of the mechanism of the dye response to potential and allow us to design optimal potentiometric indicators. This approach is illustrated by several systematic structure-property relations reported in Teisseyre et al. (2007), and exemplified in Fig. 19.4.

We now consider a class of dyes other than the styryl dyes discussed above. These dyes are based on retinal, the chromophore associated with rhodopsin found in visual systems and in bacterial rhodopsins where a retinal chromophore is bound in the membrane embedded protein. In fact studies of resonant second harmonic generation in membranes began with the retinal protein bacteriorhodopsin (Huang and Lewis 1989). However, even though all trans retinal was used in a study by the group of Yuste in Columbia (Nemet et al. 2004), there has been little effort to investigate this broad class of chromophores in terms of their second harmonic membrane voltage sensitivity.

Therefore, this was the objective of a recent study (Theer et al. 2011). That compared all trans retinal and several synthetic retinals to the styryl dye FM4-64, discussed above. This study found that the retinal chromophores had a large sensitivity to membrane potential changes, which were also quantified in terms of response kinetics. The voltage sensitivity, for example, of all trans retinal was over twice that of FM4-64. Moreover, as part of the analysis it was possible to provide information about the probe’s location and orientation inside the membrane.

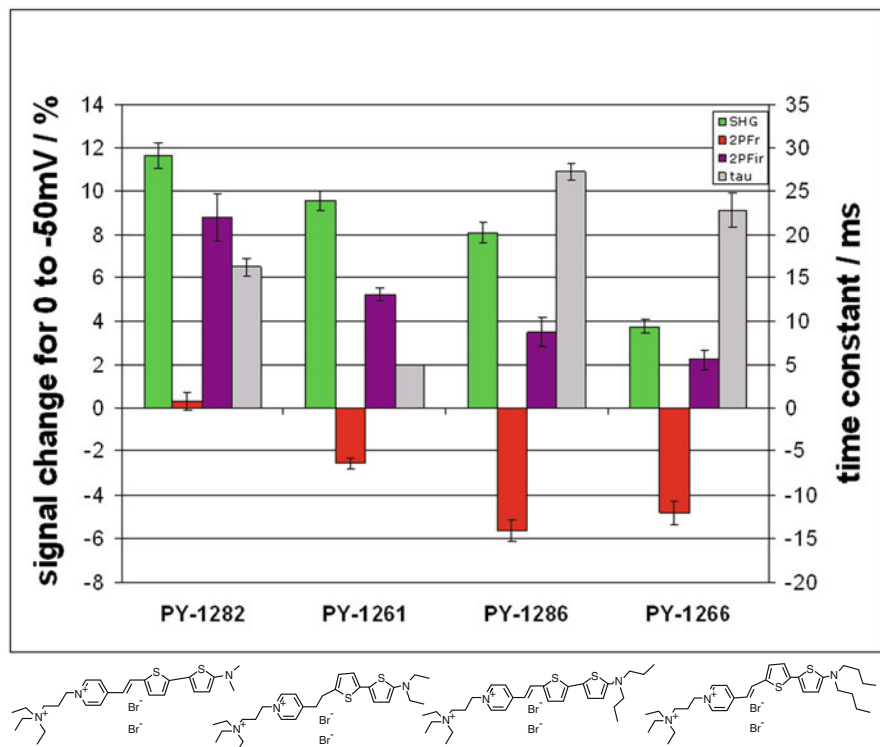


Fig. 19.4 Comparison of the effect of lipophilic tail length on the non-linear optical response of a series of amino-thiophene dyes. The incident light is from a 1,064 nm fs laser. The SHG in green was recorded at 532 nm. 2PF was recorded at emission ranges of 615–665 nm (red) and 750–850 nm (violet). The right axis refers to the SHG response time constant (gray). From Teisseyre et al. (2007). Reprinted with the permission of Journal of Biomedical Optics

The theoretical framework used in this paper is similar to that presented above in relation to Eqs. (19.1) and (19.2); it should be important for a full comparative analysis of other dyes employed for SHG studies of membrane potential sensitivity and provides a rational basis for fine tuning molecular structure to improve probe performance in the future. Specifically, they considered the case when $\chi_3 E_m$ is not small relative to χ_2 , as would be expected for a voltage drop across a 7.5 nm membrane. Under this condition these workers showed that a parabolic expression is obtained for the change in second harmonic signal versus the voltage. This is important since χ_3 normally changes more rapidly with frequency than χ_2 and thus, in order to perform a good comparison of data in this field, the effect of frequency on the signal has to be evaluated in the resonance case especially when the signal change is larger than 10 %. The effectiveness of this analysis was shown for the retinal dyes in terms of their second harmonic sensitivity as a function of voltage. In the case of all trans retinal a full analysis was possible due to the fact that the first and second order non-linear molecular hyperpolarizabilities, β and γ are known.

Therefore, a best fit based on the derived equation could be affected by adjusting the surface (E_s), dipole (E_d) and transmembrane potential (E). This analysis yielded the probe's location in the membrane and the probe's orientation in the membrane could be deduced. It was shown that a best fit of the data was obtained with the β -ionone ring of the retinal embedded in the membrane with the saturated carbon chain oriented toward the outside of the membrane.

In addition, the study demonstrated for comparison purposes that these retinal dyes in the same cell culture environment had a much faster response than FM4-64. As noted above, even though Jiang et al. 2007 reported that FM4-64 responds to voltage changes on a submillisecond timescale in the cell types they used, the Theer et al. study measure a 1.6 ms time constant in their cells. When all dyes are compared in the same cell type the retinal dyes showed an instrumentally limited response (i.e. $<100 \mu\text{s}$) unlike FM4-64.

4 Measuring SHG Response to Membrane Potential

Imaging SHG requires a microscope equipped with a mode-locked laser excitation source similar to the setup used for a 2-photon microscope (Wilson et al. 2014). Laser scanning, as in confocal microscopy, permits rapid acquisition of high resolution images. Our original non-linear microscope allowed us to produce the first high resolution SHG images, for which we coined the acronym Second Harmonic Imaging Microscopy (SHIM) (Campagnola and Loew 2003). This was an inverted microscope that used a mode locked Ti-Sapphire laser pumped with an argon ion laser to produce 120 fs pulses in the range of 720–980 nm. We have added a fiber laser to this system that has a fixed wavelength of 1,064 nm, but is extremely robust and turnkey; we have also upgraded our laser system to use a solid state pump laser. The recent availability of computer controlled integrated solid state pumped Ti-Sapphire laser systems that allow automated choice of wavelength in the entire range from 680 nm to 1080 nm, makes the laser technology both more powerful and more accessible to experimentalists without significant optics training.

The primary difference between 2-photon laser scanning microscopy and SHIM is in the detection path. Indeed, it is quite straightforward to take advantage of this difference so as to acquire both 2PF and SHIM from the same specimen simultaneously. The light paths are shown in Fig. 19.5. The key point is that because the SHG signal is coherent and co-propagates with the fundamental laser light, it is optimally collected in the transmitted light path of the microscope. A good condenser is sufficient to capture the SHG transmission. On the other hand, 2PF emanating from the focus of the laser, propagates in all directions. It is typically and most conveniently collected in the backward direction with the same objective that was used to deliver the focused laser light. Clearly, the appropriate filters need to be employed in each light path to collect the desired wavelengths and reject the transmitted or reflected fundamental laser light (not shown in Fig. 19.5). As has

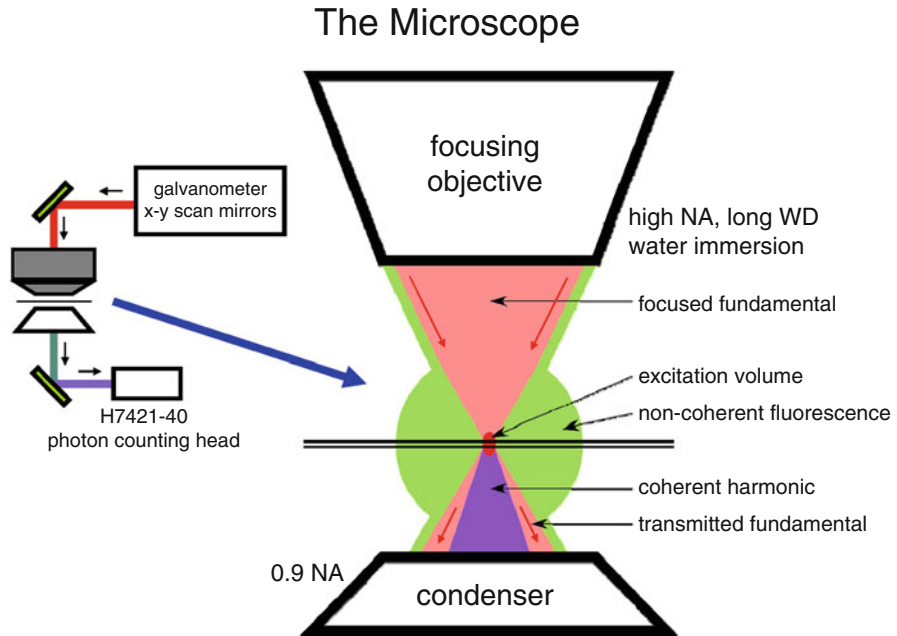


Fig. 19.5 Optical setup for non-linear optical microscopy. This arrangement is designed for simultaneous acquisition of 2PF through the backward (epi) light path and SHG through the forward (transmitted) light path. Raster scanned laser light (*red*) is focused onto the specimen with the objective and produces both 2PF (*green*) and SHG (*violet*) only at the focal plane. The 2PF emanates in all directions and a portion is collected by the objective in the backward direction, as is common in most fluorescence microscopes. For optical recording from brain slices, the objective should be water immersion and have a long working distance. It also should have good transmittance in the entire range from 700 to 1,100 nm. The SHG co-propagates with the fundamental laser light and both are collected by a high numerical aperture condenser. A short pass reflector combined with a band pass filter at half the wavelength of the fundamental laser beam is inserted before the detector to reject the fundamental and pass the SHG

been emphasized previously, the SHG signal occurs at precisely $\frac{1}{2}$ the wavelength of the fundamental; therefore the choice of filter will be dependent on the laser wavelength. This is not the case for 2PF, as the emission spectrum is independent of the exciting wavelength.

Depending on the needs of the experiment, dye can be applied either from the bathing medium or internally through the patch pipette. The former can be used to stain the entire preparation and the latter allows the experimentalist to target a single neuron. As has been discussed above, a non-centrosymmetric distribution of dye is required for SHG. Consequently if the stained membranes in a multicellular preparation are too close to each other, the SHG signal will be weak. For dyes applied to the outside, therefore, it would be important that they preferentially stain a subpopulation of cells. But a better application of SHG to membrane potential imaging might be for single cell measurements. Dye applied through a patch pipet

will stain not just the plasma membranes, but also internal membranous organelles—most notably the endoplasmic reticulum—this produces large background signal when measuring fluorescence. Importantly, however, the SHG signal from the endoplasmic reticulum is very weak compared to that from the plasma membrane. This is because the convoluted structure of the endoplasmic reticulum effectively creates a centrosymmetric array of dye molecules. Thus, SHIM of cells stained internally primarily show plasma membrane intensity, while 2PF of the same dye in these cells display huge background from endoplasmic reticulum fluorescence. Indeed, the successful test cases in the Webb and Yuste labs were all measurements of single isolated cells (Dombeck et al. 2005; Nuriya et al. 2006; Sacconi et al. 2006). Most recently, several other labs have measured voltage-dependent SHG from axons in isolated neurons and from neurons in brain slice preparations (Nuriya and Yasui 2010; Rama et al. 2010) Fig. 19.6, taken from Dombeck et al. 2005, shows SHG from hippocampal neurons in a brain slice. In these experiments, FM4-64 is applied through a whole cell patch pipet. Very little intensity is observed from the interior of the cells, although 2PF images of the same cells (see Figure 1 of Dombeck et al. 2005) shows significant fluorescence from internal membranes. Figure 19.6 also shows optically recorded action potentials from the SHG intensity recorded on patches of the membrane using the laser scanning line scan mode. Notably, 55 scans were averaged to obtain the data in

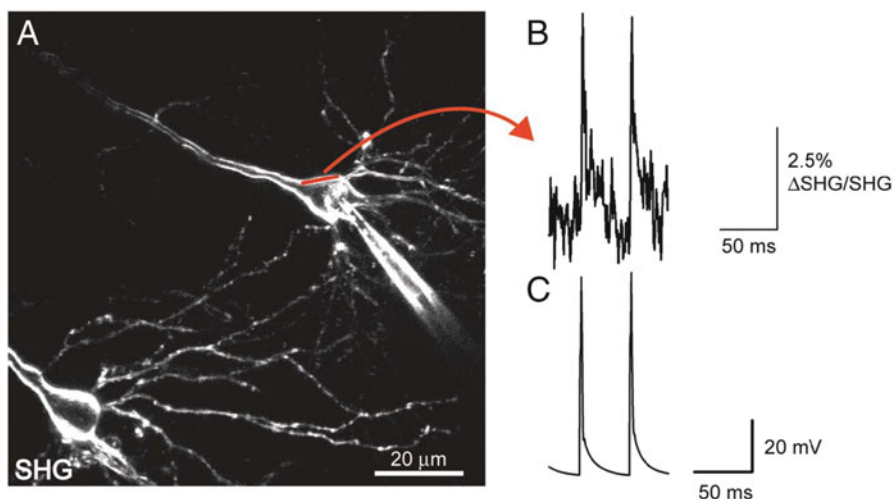


Fig. 19.6 Fast SHG line scan recording of elicited APs in brain slice. (a) To show recording of action potentials (APs) with SHG, this neuron was patch clamped and filled with FM4-64. Straight red line represents scanned line where elicited APs were recorded optically by integrating over the width. (b) SHG recording of APs with S/N of 7–8. This intensity plot of SHG emission vs. time is obtained from averaged line scans (1,200 lines/s) of the line denoted in a. $n = 55$ line scans were averaged. (c) Average current-clamp trace of elicited APs recorded optically in b. This figure was taken from Dombeck et al. (2005) and is reprinted by permission of the authors and the Journal of Neurophysiology

Fig. 19.6. Thus, despite the large signal to background ratio and despite the good sensitivity of the signal to membrane potential, the low intensity of the SHG signal requires significant averaging to overcome the poor signal to noise ratio of SHG measurements.

5 Conclusion

In this chapter we have reviewed the current status of second harmonic generation as a new modality for optical recording of membrane potential. The special properties of SHG were described, followed by an exposition of their origins based on both qualitative physical arguments and quantitative theory. We summarized the ways that SHG from dye-stained membranes could be modulated by membrane potential and showed how such an experiment is performed. The largest potentiometric sensitivity of SHG from a dye stained membrane is approximately 40 %/100 mV, which is significantly higher than the best fluorescence recordings. SHG also shows advantages for recording from internally stained single cells in brain slice preparations because there is no background signal from internal organelle membranes, as there is for similar fluorescence-based experiments. However, a significant impediment to the practical application of SHG for optical recording is the small number of photons that are produced compared to fluorescence. We and other will continue efforts to design and synthesize new SHG dyes with improved properties—most importantly, increased SHG efficiency. We expect that as the dyes are improved and the SHG methods for measuring membrane potential are optimized, recording of membrane potential from the membranes of internally stained cells will become the dominant application for SHG-based optical recording.

Acknowledgment We are indebted to the many talented students and colleagues who have participated in the development of SHG imaging in our laboratories over the last 20 years. This work was supported by NIH EB001963.

References

- Araya R, Jiang J, Eiselthel KB, Yuste R (2006) The spine neck filters membrane potentials. *Proc Natl Acad Sci U S A* 103:17961–17966
- Araya R, Nikolenko V, Eiselthel KB, Yuste R (2007) Sodium channels amplify spine potentials. *Proc Natl Acad Sci U S A* 104:12347–12352
- Ben-Oren I, Peleg G, Lewis A, Minke B, Loew LM (1996) Infrared nonlinear optical measurements of membrane potential in photoreceptor cells. *Biophys J* 71:1616–1620
- Bianchini P, Diaspro A (2008) Three-dimensional (3D) backward and forward second harmonic generation (SHG) microscopy of biological tissues. *J Biophotonics* 1:443–450
- Bouevitch O, Lewis A, Pinevsky I, Wuskell JP, Loew LM (1993) Probing membrane potential with non-linear optics. *Biophys J* 65:672–679

- Campagnola P, Loew LM (2003) Second-harmonic imaging microscopy for visualizing biomolecular arrays in cells, tissues and organisms. *Nat Biotechnol* 21:1356–1360
- Campagnola PJ, Clark HA, Mohler WA, Lewis A, Loew LM (2001) Second harmonic imaging microscopy of living cells. *J Biomed Opt* 6:277–286
- Campagnola PJ, Wei M-d, Lewis A, Loew LM (1999) High resolution optical imaging of live cells by second harmonic generation. *Biophys J* 77:3341–3349
- Clark HA, Campagnola PJ, Wuskell JP, Lewis A, Loew LM (2000) Second harmonic generation properties of fluorescent polymer encapsulated gold nanoparticles. *J Am Chem Soc* 122:10234–10235
- Cole JM, Kreiling S (2002) Exploiting structure/property relationships in organic non-linear optical materials: developing strategies to realize the potential of TCNQ derivatives. *CrystEngComm* 4:232–238
- Conboy JC, Richmond GL (1997) Examination of the electrochemical interface between two immiscible electrolyte solutions by second harmonic generation. *J Phys Chem B* 101:983–990
- Denk W, Strickler JH, Webb WW (1990) Two-photon laser scanning fluorescence microscopy. *Science* 248:73–76
- Dirk CW, Twieg RJ, Wagniere J (1986) The Contribution of Pi Electrons to Second Harmonic Generation in Organic Molecule. *J Am Chem Soc* 108:5387–5395
- Dombeck DA, Blanchard-Desce M, Webb WW (2004) Optical recording of action potentials with second-harmonic generation microscopy. *J Neurosci* 24:999–1003
- Dombeck DA, Sacconi L, Blanchard-Desce M, Webb WW (2005) Optical recording of fast neuronal membrane potential transients in acute mammalian brain slices by second-harmonic generation microscopy. *J Neurophysiol* 94:3628–3636
- Fluhler E, Burnham VG, Loew LM (1985) Spectra, membrane binding and potentiometric responses of new charge shift probes. *Biochemistry* 24:5749–5755
- Freund I, Deutsch M, Sprecher A (1986) Connective tissue polarity. Optical second-harmonic microscopy, crossed-beam summation, and small-angle scattering in rat-tail tendon. *Biophys J* 50:693–712
- Huang J, Lewis A (1989) Determination of the absolute orientation of the retinylidene chromophore in purple membrane by a second harmonic interference technique. *Biophys J* 55:835–842
- Huang JY, Lewis A, Loew LM (1988) Non-linear optical properties of potential sensitive styryl dyes. *Biophys J* 53:665–670
- Jiang J, Eisenthal KB, Yuste R (2007) Second harmonic generation in neurons: electro-optic mechanism of membrane potential sensitivity. *Biophys J* 93:L26–L28
- Millard AC, Campagnola PJ, Mohler W, Lewis A, Loew LM (2003a) Second harmonic imaging microscopy. In: Marriott G, Parker I (eds) *Methods in enzymology*, vol. 361B. Academic, San Diego, pp 47–69
- Millard AC, Jin L, Lewis A, Loew LM (2003b) Direct measurement of the voltage sensitivity of second-harmonic generation from a membrane dye in patch-clamped cells. *Opt Lett* 28:1221–1223
- Millard AC, Jin L, Wei M-d, Wuskell JP, Lewis A, Loew LM (2004) Sensitivity of second harmonic generation from styryl dyes to trans-membrane potential. *Biophys J* 86:1169–1176
- Millard AC, Jin L, Wuskell JP, Boudreau DM, Lewis A, Loew LM (2005a) Wavelength- and time-dependence of potentiometric non-linear optical signals from styryl dyes. *J Membr Biol* 208:103–111
- Millard AC, Lewis A, Loew LM (2005b) Second harmonic imaging of membrane potential. In: Yuste R, Konnerth A (eds) *Imaging in neuroscience and development*. Cold Spring Harbor Laboratory Press, Cold Spring Harbor, pp 463–474
- Mohler W, Millard AC, Campagnola PJ (2003) Second harmonic generation imaging of endogenous structural proteins. *Methods* 29:97–109
- Moreaux L, Pons T, Dambrin V, Blanchard-Desce M, Mertz J (2003) Electro-optic response of second-harmonic generation membrane potential sensors. *Opt Lett* 28:625–627

- Moreaux L, Sandre O, Blanchard-desce M, Mertz J (2000a) Membrane imaging by simultaneous second-harmonic generation and two-photo microscopy. *Opt Lett* 25:320–322
- Moreaux L, Sandre O, Mertz J (2000b) Membrane imaging by second harmonic generation microscopy. *J Opt Soc Am B* 17:1685–1694
- Morley JO (1988) Non-linear optical properties of organic molecules. 7. Calculated hyperpolarizabilities of azulenes and sesquifulvalene. *J Am Chem Soc* 110:7660–7663
- Nemet BA, Nikolenko V, Yuste R (2004) Second harmonic imaging of membrane potential of neurons with retinal. *J Biomed Opt* 9:873–881
- Nicoud JF, Twieg RJ (1987) Design and synthesis of organic molecular compounds for efficient second-harmonic generation. In: Chemla DS, Zyss J (eds) *Nonlinear optical properties of organic molecules and crystals*, vol. 1. Academic, Orlando, pp 227–296
- Nuriya M, Jiang J, Nemet B, Eisenthal KB, Yuste R (2006) Imaging membrane potential in dendritic spines. *Proc Natl Acad Sci U S A* 103:786–790
- Nuriya M, Yasui M (2010) Membrane potential dynamics of axons in cultured hippocampal neurons probed by second-harmonic-generation imaging. *J Biomed Opt* 15:020503
- Pons T, Moreaux L, Mongin O, Blanchard-Desce M, Mertz J (2003) Mechanisms of membrane potential sensing with second-harmonic generation microscopy. *J Biomed Opt* 8:428–431
- Rama S, Vetrivel L, Semyanov A (2010) Second-harmonic generation voltage imaging at subcellular resolution in rat hippocampal slices. *J Biophotonics* 3:784–790
- Sacconi L, Dombek DA, Webb WW (2006) Overcoming photodamage in second-harmonic generation microscopy: real-time optical recording of neuronal action potentials. *Proc Natl Acad Sci U S A* 103:3124–3129
- Sheppard C, Kompfner R, Gannaway J, Walsh D (1977) *IEEE J Quant Electron* 13D:100E
- Teisseyre TZ, Millard AC, Yan P, Wuskell JP, Wei M-d, Lewis A, Loew LM (2007) Non-linear optical potentiometric dyes optimized for imaging with 1064 nm light. *J Biomed Opt* 12:044001–044008
- Theer P, Denk W, Sheves M, Lewis A, Detwiler PB (2011) Second-harmonic generation imaging of membrane potential with retinal analogues. *Biophys J* 100:232–242
- Williams DJ (1984) Organic polymeric and non-polymeric materials with large optical non-linearities. *Angew Chem Int Ed Engl* 23:690–703
- Wilson SA, Millard A, Lewis A, Loew LM (2014) Monitoring membrane potential with second-harmonic generation. *Cold Spring Harb Protoc* 2014:643–654
- Yan ECY, Liu Y, Eisenthal KB (1998) New method for determination of surface potential of microscopic particles by second harmonic generation. *J Phys Chem B* 102:6331–6336
- Yan P, Millard AC, Wei M, Loew LM (2006) Unique contrast patterns from resonance-enhanced chiral SHG of cell membranes. *J Am Chem Soc* 128:11030–11031
- Yan P, Xie A, Wei M-d, Loew LM (2008) Amino(oligo)thiophene-based environmentally sensitive biomembrane chromophores. *J Org Chem* 73:6587–6594
- Zhou W-L, Yan P, Wuskell JP, Loew LM, Antic SD (2007) Intracellular long wavelength voltage-sensitive dyes for studying the dynamics of action potentials in axons and thin dendrites. *J Neurosci Methods* 164:225–239